Enantiopure, luminescent, cyclometalated Ir(iii) complexes with N-heterocyclic carbene-naphthalimide chromophore: design, vibrational circular dichroism and TD-DFT calculations

Antoine Groué, Eve Montier-Sorkine, Yaping Cheng, Marie Noelle Rager, Marion Jean, Nicolas Vanthuyne, Jeanne Crassous, Amalia Lopez, Alejandra Saavedra Moncada, Andrea Barbieri, et al.

Dalton Transactions

PAPER

Enantiopure, Luminescent, Cyclometalated Ir(III) Complexes with *N*-Heterocyclic Carbene-Naphthalimide Chromophore: Design, Vibrational Circular Dichroism and TD-DFT Calculations

Received 00th January 20xx,
Accepted 00th January 20xx

DOI: 10.1039/x0xx00000x

www.rsc.org/

Antoine Groué,[a] Eve Montier-Sorkine,[a] Yaping Cheng,[a] Marie Noelle Rager,[b] Marion Jean,[c] Nicolas Vanthuyne,[c] Jeanne Crassous [d]* Amalia C. Lopez,[f] Alejandra Saavedra Moncada,[e] Andrea Barbieri, [e] Andrew L. Cooksy,[f] and Hani Amouri,[a]*

A series of chiral cyclometalated iridium complexes of the type [Ir(C^N)$_2$(C^C:)], {(C^N) = ppy (**2**); dfppy (**3**)} featuring a naphthalimide *N*-heterocyclic carbene ligand (C^C:) = (Naphthalimide-NHC) are described and fully characterized. The racemic complexes *rac*-**2** and *rac*-**3** were resolved via chiral column chromatography techniques into their corresponding enantiopure species Δ-**2** Λ-**2**, Δ-**3**, Λ-**3** as confirmed by their CD curves. This unique class of molecules containing organic and inorganic chromophores might be used as a platform to probe the stereochemical effect on the photophysical properties. Vibrational circular dichroism (VCD) was used as an important tool to assign successfully the stereochemistry of the enantiomers. TD-DFT calculations are also advanced to support the experimental studies and to rationalize the observed results.

Introduction

Cyclometalated iridium complexes have attracted much attention due to their remarkable photoluminescent properties[1] and continue to be the systems of choice to construct efficient luminescent devices.[2] For instance, such compounds are amenable to important applications, among others as active components in organic light-emitting diodes (OLEDs),[3] single layer emitting diodes, unimolecular oxygen sensors[4-6] and as biological labeling reagents.[7] These d^6 complexes are attractive in photochemical applications, because they generally have long–lived excited states and high luminescence efficiencies.[8] These properties are due to efficient intersystem crossing between the singlet and triplet excited states brought about by the strong spin–orbit coupling of the Ir(III) metal ion (coupling constant, ζ_{Ir} = 3,909 cm^{-1}).[9] In addition, the incorporation of N-heterocyclic carbene ligands around the coordination sphere of the iridium center contributes also to improve the stability and efficiency of the iridium complexes.[10]

However, while these investigations have been mainly carried out on racemic compounds, only a few studies by *Gladysz, Ye and Meggers* have been conducted on the enantiopure version of octahedral cyclometalated iridium compounds and related metal complexes.[11-17] The reason for this lag is related to the difficulty of resolving the racemic compounds into their corresponding enantiomers.[18-20] It should be mentioned that enantiopure compounds tend to pack differently from the racemic complexes and hence one might expect that stereochemistry could affect the photophysical properties. For instance, the racemic and enantiopure complexes of cationic cyclometalated iridium compounds [Ir(C^N)$_2$(dtBubpy)][PF$_6$] {C^N = ppy, mesppy} were reported to show different emissions in thin films.[21] On the other hand some of us demonstrated that enantiopure Pt(terpy) complexes containing chiral organometallic ligands display different emission properties in the solid state when compared to their corresponding racemic species.[22] In previous work we designed a family of luminescent cyclometalated iridium compounds with *N*-heterocyclic carbene ligands attached to an organic naphthalimide chromophore.[23, 24] All complexes were deep red emitters (CIE 1931 0.71, 0.29) with good quantum yields, long lifetimes in liquid solution at room temperature and displayed broad emission bands extending beyond 700 nm.[25] While cyclometalated iridium complexes commonly emit from a ^{3}MLCT state, the presence of the organic naphthalimide chromophore dramatically modified the nature of the excited states from ^{3}MLCT to mostly naphthalimide centred ^{3}LC.

In this work we describe the synthesis of a novel class of luminescent cyclometalated iridium complexes with NHC-

[a] Sorbonne Universités, UPMC Univ Paris 06, Université Pierre et Marie Curie, Institut Parisien de Chimie Moléculaire (IPCM) UMR 8232, 4 place Jussieu, 75252 Paris cedex 05, France: hani.amouri@sorbonne-universite.fr
[b] Chimie ParisTech, PSL University, NMR Facility, 11, rue Pierre et Marie Curie, 75005 Paris, France. [c] Aix Marseille Univ, CNRS, Centrale Marseille, iSm2, Marseille, France. [d] Institut des Sciences Chimiques de Rennes UMR 6226 Institut de Physique de Rennes, UMR 6251 CNRS Université de Rennes 1 Campus de Beaulieu, 35042 Rennes, France: E-mail: jeanne.crassous@univ-rennes1.fr. [e] Istituto per la Sintesi Organica e la Fotoreattività, Consiglio Nazionale delle Ricerche, Via Gobetti 101, 40129 Bologna, Italy. [f] Department of Chemistry, San Diego State U., San Diego CA 921821030, USA.

† Electronic Supplementary Information (ESI) available: (^{1}H- and ^{13}C)-NMR spectra of prepared compounds, Resolution techniques, UV/vis and ECD spectra are given as well as their simulation. Detailed TD-DFT calculations of all transitions are also included.

naphthalimide chromophore **2-3**. An *n*-butyl group is now attached to the nitrogen of the carbene unit in order to increase the stability and solubility of these complexes to facilitate their resolution on chiral column chromatography to the corresponding *Δ*- and *Λ*-enantiomer (Figure 1). All compounds were found to be luminescent in the far red/NIR region of the electromagnetic spectrum. Interestingly replacement of the ppy in complex **2** by dfppy increases the quantum yield by 10-fold. Moreover, the photophysical properties of the racemic and enantiopure compounds were investigated in solution and thin films. Vibrational circular dichroism was used as a valuable tool to ascertain the configuration at the metal centre in the enantiopure series. Computations allowed us to support the experimental results. This work paves the way to study and to probe the influence of stereochemistry on the luminescent properties.

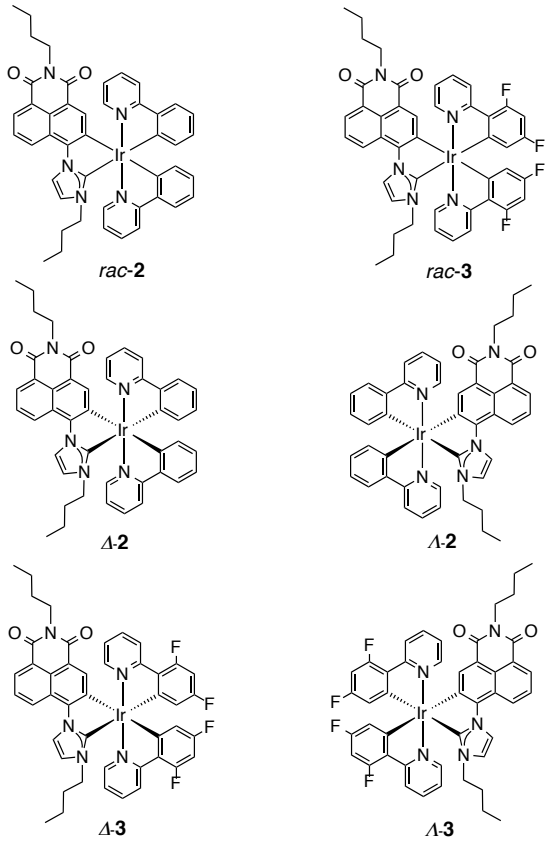

Figure 1. Complexes described in this work.

Results and discussion

Syntheses and characterization

The synthesis of the ligands and racemic compounds *rac*-**2** and *rac*-**3** was performed following a synthetic procedure developed by some of us.[23-25] The imidazole-naphthalimide (IMD-NI) chromophore was alkylated with *n*BuI in CH_3CN under reflux to give the imidazolium salt **1** in 93% yield (Scheme 1). The ^{1}H NMR spectra recorded in $CDCl_3$ show a typical unshielded signal of the C1 proton of the imidazole moiety at 10.30 ppm. The $[Ir(C^N)_2(C^C:)]$ complexes *rac*-(**2**-**3**) were obtained by heating the imidazolium salt (**1**) with the chosen chloro-bridged Ir(III) dimeric precursor compound $[Ir(C^N)_2Cl]_2$ (C^N = ppy, dfppy) and Ag_2O in refluxing 1,2-dichloroethane.[25] All compounds were fully characterized. For instance, the ^{1}H NMR spectra of *rac*-**2** recorded in CD_2Cl_2 confirmed the absence of the signal at δ 10.30 ppm attributed to the imidazolium salt starting material. Furthermore, 16 multiplets in the range of δ 6.3-8.7 ppm are visible, which show the non-equivalence of the arene rings of the (C^N) ligands, as expected for complexes with lack of symmetry. The 2D-NOESY spectra of **2** and **3** show correlations between one (C^N) ligand and the naphthalimide moiety, between the second (C^N) ligand and the imidazole moiety, as well as between the two (C^N) ligands confirming the structure of the molecules. Moreover, the two methylene protons of the *n*-Bu group on the NHC become diastereotopic after coordination and appear as two doublet of doublet of doublets (δ 3.46 and 3.67 ppm) for *rac*-**2** and (δ 3.49 and 3.64 ppm) for *rac*-**3** relative to the starting material, in which these two protons are equivalent and appear as a triplet δ 4.66 ppm. The ^{1}H-NMR of *rac*-**3** displays 12 multiplets and appear as two sets of resonances between 5.7-8.7 ppm. Moreover, the $^{19}F\{^1H\}$-NMR spectrum of *rac*-**3** recorded in CD_2Cl_2 showed the presence of four distinct doublets in the area of δ -107 to -111 ppm which confirms the lack of symmetry in these heteroleptic cyclometalated Ir(III) carbene complexes. Full characterization is given in the experimental section.

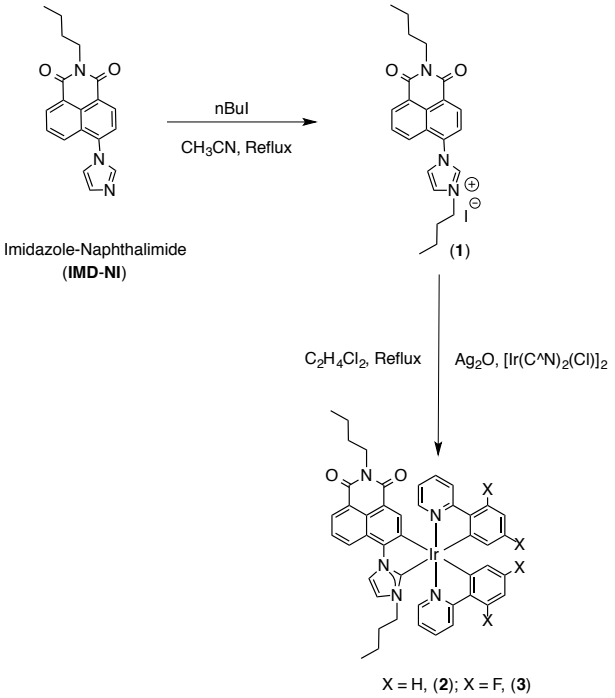

Scheme 1. Synthesis of the cyclometalated iridium carbene racemic compounds *rac*-(**2**-**3**).

The ^{1}H-NMR of these compounds remain unchanged even after several days in solution suggesting that the presence of the *n*Bu group at the carbene unit increases the stability and the solubility of our compounds in solution and makes such compounds amenable for chiral resolution. Thus, the enantiopure versions of the above compounds *Δ*-**2**, *Λ*-**2** and *Δ*-**3**, *Λ*-**3** were obtained by resolving the racemic complexes $[Ir(ppy)_2(C^C:)]$ *rac*-**2** and $[Ir(dfppy)_2(C^C:)]$ *rac*-**3** using chiral column chromatography. Compounds **2** and **3** were resolved

respectively on Chiralpak IE column using heptane/ethanol/ dichloromethane (80/10/10) mixture as eluent. The optical rotations of both enantiomers were monitored as well (experimental details of their resolution are given in the SI). At same concentration, the ^{1}H-NMR spectra of the *rac*-**2**, *Δ*-**2**, *Λ*-**2** and *rac*-**3**, *Δ*-**3**, *Λ*-**3** were identical respectively.

In the absence of crystal structure of the enantiomeric species, the absolute configuration was assigned using VCD techniques and confirmed by TD-DFT calculations (vide infra).

The CD spectra of the both enantiomers of **2** and **3** are given in Figures 2 and 3.

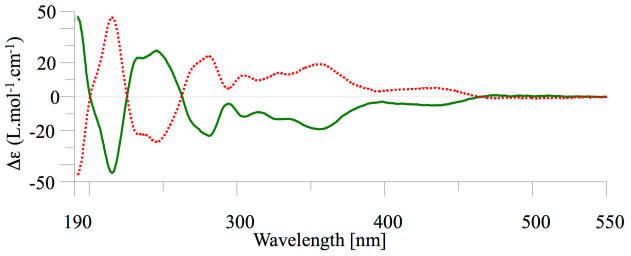

Fig 2. CD spectra of *Δ*-**2** (green) and *Λ*-**2** (red) recorded in CH3CN at 0.19mM**.**

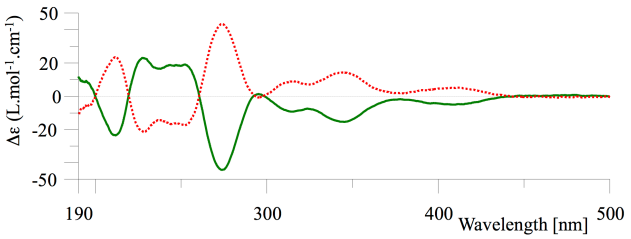

Fig 3. CD spectra of *Δ*-**3** (green) and *Λ*-**3** (red) recorded in CH_3CN at 0.2mM.

Having successfully prepared the racemic complexes [Ir(ppy)$_2$(C^C:)] (**2**) and [Ir(dfppy)$_2$(C^C:)] (**3**) and the related optically active compounds *Δ*-**2**, *Λ*-**2** and *Δ*-**3**, *Λ*-**3**. We examined first their optical properties in solution and solid state (vide infra).

Photophysical properties.

Absorption

The main absorption features of the iridium(III) complexes *rac*-**2**, *rac*-**3** and *Δ*-**2**, *Λ*-**2** and *Δ*-**3**, *Λ*-**3** in acetonitrile solution at room temperature are summarized in Table 1. The relevant spectra are shown in Figures S20, S21 (see supporting information).

As reported previously, the IMD-NI organic chromophore displays a broad and relatively intense absorption band centered at about 340 nm with ε_{max} ~18,000 M^{-1} cm^{-1}.[23-25] This band is attributed to $^1\pi,\pi^*$ transitions with a strong intramolecular charge transfer (ICT) character, as commonly observed for this class of molecules.[26]

The absorption spectra of the iridium(III) complexes *rac*-**2**, *rac*-**3** and *Δ*-**2**, *Λ*-**2** and *Δ*-**3**, *Λ*-**3** show a series of strong absorption bands in the UV region associated with the naphthalimide and aryl-pyridine ligands, and an envelope of less intense bands above 350 nm (Figures. S17-S18). The absorption above 400 nm is predominantly attributed to metal-to-ligand charge transfer (MLCT) transitions with a strong ligand-centered (LC) contribution from the carbene ligand. The long tail of moderate intensity is attributed to the direct singlet-triplet transition induced by the large spin-orbit coupling (SOC) of the Ir atom.[9]

Emission

The emission spectra of the racemic iridium(III) complexes *rac*-**2**, *rac*-**3** and the relevant enantiopure species *Δ*-**2**, *Λ*-**2** and *Δ*-**3**, *Λ*-**3** in CH_3CN solution are reported in Figures S20-S21 while the main photophysical parameters are collected in Table 2.

All iridium(III) complexes are luminescent in de-aerated solution at room temperature and have a very similar emission shape. The ppy derivative **2** displays a slightly red-shifted emission with respect to the relevant dfppy analogue **3**. This behaviour is also observed in the relevant parent complexes Ir(ppy)$_3$ and Ir(dfppy)$_3$ because of the electron withdrawing effect of the fluorine atom that stabilize the HOMO level, only slightly affecting the LUMO level.[1] The latter shows the highest quantum yield in the series, roughly 10-times higher than the ppy derivative with longer lifetime (Table 2). The nature of the emission can be attributed to mixed ^{3}MLCT/^{3}LC excited states, as also supported by the value of the radiative constant $k_r = \phi / \tau$, which is on the order of 10^4 s^{-1}. Previous study using DFT calculations on related complexes with *Me*-group at the carbene unit confirmed a more pronounced ^{3}LC character of emitting states, with a negligible ^{3}MLCT contribution. As both series of complexes display similar radiative constant values, the observed variation in the quantum yield should be predominantly ascribable to considerably different non-radiative deactivation pathways ($k_{nr} \approx 1\times10^6$ and 6×10^4 s^{-1} for **2** and **3**, respectively).[25]

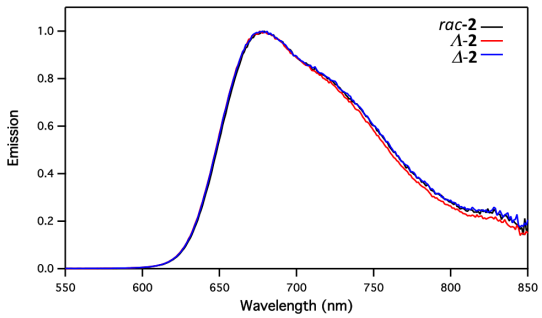

Fig 4. Normalized emission spectra of the *rac*-**2** and the *Λ*-**2**, *Δ*-**2** enantiomers as powder at room temperature.

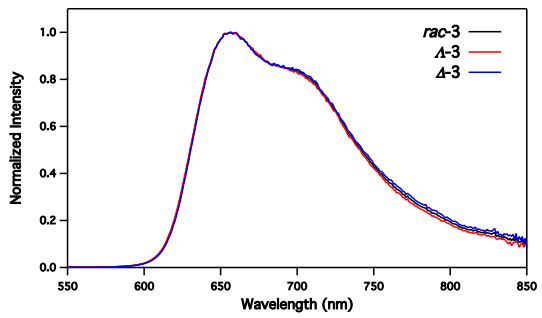

Fig 5. Normalized emission spectra of the *rac*-**3** and the *Λ*-**3**, *Δ*-**3** enantiomers as powder at room temperature

The pure enantiomers do not display any significant difference in luminescence behaviour with respect to that of the racemic mixtures (Figures. S20-S21). Moreover, the emission properties of the above compounds (racemic and enantiopure) were also investigated in powder thin films. The results show a similar trend with a major band at 685 nm for the *rac*-**2**, *Λ*-**2**/*Δ*-**2** and at 650 nm for *rac*-**3**, *Λ*-**3**/*Δ*-**3** (Figures 4 and 5). The data in solid state show also almost the same kind of emissions for the racemic and enantiopure species**.** Our result is different from that reported for the octahedral iridium complexes.[21] We feel in our case no aggregation among the individual molecules is occurring so that racemic or enantiomer species behaved as single molecules even in solid state. Perhaps this might arise from the *n*Bu group, which does not bring rigidity to the system although it increases their solubility and stability for chiral column resolution. We then explored the vibrational circular dichroism technique in order to assign the absolute configuration of the enantiopure species.[27, 28]

Table 1. Main absorption parameters [a]

	λ, nm (ε, 10^3 M^{-1}·cm^{-1})
rac-**2**	361 (16.0), 395sh (10.6), 420sh (7.7), 470sh (2.9)
Λ-**2**	361 (16.3), 395sh (11.4), 420sh (8.3), 470sh (3.1
Δ-**2**	361 (15.6), 395sh (10.9), 420sh (8.0), 470sh (3.0)
rac-**3**	353 (15.2), 375sh (12.8), 405sh (7.6), 445sh (4.4)
Λ-3	353 (15.5), 375sh (13.6), 405sh (8.4), 445sh (4.2)
Δ-3	353 (14.6), 375sh (12.8), 405sh (7.9), 445sh (4.0)

[a] In CH_3CN solution at room temperature.

Table 2. Main emission parameters

	Emission[a]			Emission[b]	
	λ, nm	ϕ, %	τ, μs	λ, nm	τ, μs
rac-**2**	685	1.1	0.8	678	7.1
Λ-**2**	685	0.9	0.8	678	7.1
Δ-**2**	685	0.9	0.8	678	7.1
rac-**3**	650	12	14.5	656	7.6
Λ-**3**	650	11.8	14.5	656	7.6
Δ-**3**	650	12.4	14.6	656	7.5

[a] In de-aerated CH_3CN solution at room temperature. [b] As powder at room temperature.

Vibrational Circular Dichroism

Vibrational circular dichroism (VCD) spectroscopy[29] is a chiroptical technique operating in the infrared (IR) domain, which is useful for determining the absolute configuration (AC) of small molecules and is complementary to other techniques such X-ray diffraction analysis. The IR and VCD spectra of *Δ*-**3** and *Λ*-**3** complexes are displayed in Figure 6A. Both complexes exhibit similar IR spectra together with clear VCD patterns. The VCD spectrum appears very rich, with almost all IR bands that are active in VCD. Interestingly, the IR and VCD spectra closely resemble those of FIrpic complex (see Figure 6B) which were reported by Longhi, Cannazza et al. in 2016.[30] In particular, the very intense (−,+) couplet found at 1633-1638 cm^{-1} for the *Λ* complex was attributed to C-C stretchings of the two difluorophenyl rings, and is a clear fingerprint of the *Λ* configuration at the iridium. This assignment is in full agreement with our complex which exhibits the same (−,+) couplet at 1591-1601 cm^{-1} for the *Λ*-**3** enantiomer. Other (−,+) couplets are found for *Λ*-**3** at 1468-1476 and 1156-1162 cm^{-1}. Similar bisignate responses were recognized as vibrational exciton couplets.[31]. Note that such types of chiral cycloiridiated complexes always exhibit similarities in their VCD.[32, 33].

We have also tried to measure circularly polarized luminescence (CPL). Unfortunately, although the complexes are emissive, our attempts to measure CPL activity failed, probably due to the near-IR region detection which is known to be less sensitive.

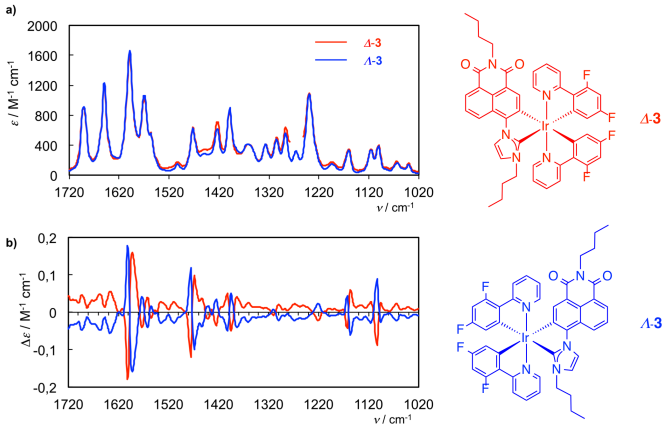

Figure 6A. Experimental IR (a) and (b) VCD spectra of complex *Δ*-**3** (red) and *Λ*-**3** (blue) in CD_2Cl_2. The half-sum has been used as the baseline.

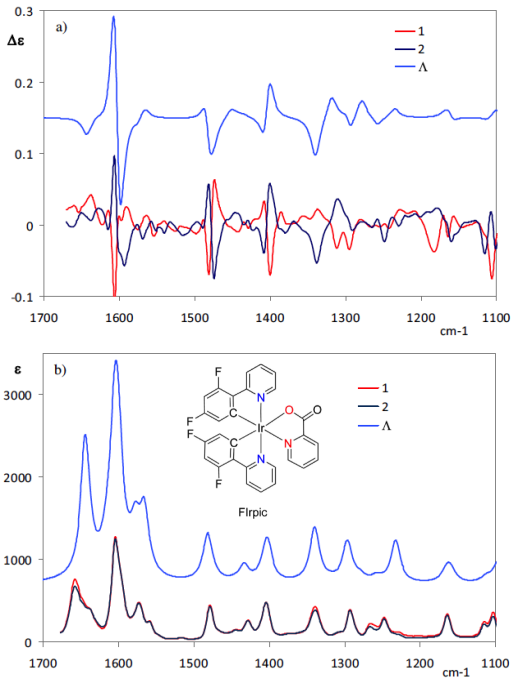

Figure 6B. Comparison of experimental VCD (a) and experimental IR (b) spectra enantiomers **1** and **2** of FIrpic with the corresponding calculated spectra of the *Λ* enantiomer. Adapted from reference [30].

DFT and TD-DFT Calculations

We carried out a B3LYP/cc-pVDZ[34-37] optimization and harmonic frequency analysis of gas-phase *Λ*-**2** and *Λ*-**3**, for comparison to the experimental IR and VCD spectra. These calculations were carried out using the Gaussian 16 suite of programs,[38] using a harmonic approximation for the vibrational energies. These tend to overestimate the transition wavenumbers by roughly 2%, which is 20—40 cm^{-1} in the range of these spectra. We would like to calculate anharmonic corrections as well, but this is a large system and those calculations are challenging.

Initial calculations with a much smaller LANL2DZ basis set[39] had many points of comparison to the experimental spectra, but there were still several ambiguities because the molecule is large and the IR spectrum is dense. The cc-pVDZ basis set gave much better agreement with experiment, and between the IR and VCD spectra we believe that we can assign with confidence 23 transitions in the region from 1000—1800 cm^{-1}. We have labelled the assigned transitions in the spectra by letters, as shown in Figure 7. A given letter refers to the same peaks in the IR and VCD spectra. In many cases, there are weaker overlapping peaks, which we do not identify here, and in others there are two unresolved peaks in the IR spectrum that can be distinguished only because they have opposite phases in the VCD spectra (C and D, H and I). Table 3 compares the experimental and calculated values, and also provides a rough description of the vibrational modes that correspond to the calculated values.

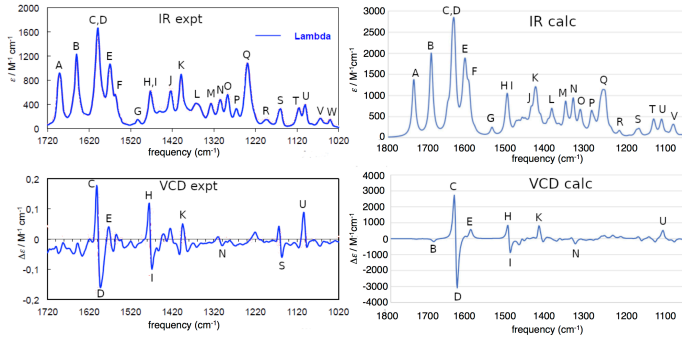

Figure 7. Experimental (left) and Calculated (right) Harmonic IR and VCD Spectra for *Λ*-**3** between roughly 1000 cm^{-1} and 1800 cm^{-1}.

Table 3. Experimental and B3LYP/cc-pVDZ/COSMO IR and VCD Spectra Assignments**.**

Label	$\nu_{calc.}$ (cm^{-1})	$\nu_{exp.}$ (cm^{-1})	Mode assignment
A	1735.3	1692	C=O sym str
B	1691.4	1651	C=O anti str
C	1638.3	1602	dfppy C=C str
D	1633.2	1595	dfppy C=C str
E	1604.9	1572	naphthalimide C=C str
F	1595.9	1563	pyridine C=C str
G	1538.4	1505	naphthalimide C=C str, C-H wag
H	1502.7	1476	pyridine C=C str, C-H wag
I	1499.4	1471	pyridine C=C str, C-H wag
J	1440.0	1425	imidazole, alkyl C-H scissors
K	1425.5	1400	dfppy C-H wag
L	1387.8	1364	butyl C-H rock
M	1352.9	1328	naphthalimide C-H wag
N	1333.8	1307	naphthalimide C-H wag
O	1314.4	1288	pyridine C-H wag
P	1287.8	1268	alkyl C-H rock
Q	1252.7	1240	global C-H wag
R	1217.1	1195	global C-H wag
S	1167.4	1152	dfppy C-H scissors
T	1132.1	1118	naphthalimide C-H scissors
U	1111.0	1101	dfppy C-H scissors
V	1079.7	1065	naphthalimide C-H scissors
W	1046.5	1040	pyridine ring bend

The electronic spectra of the two compounds were also simulated using TD-DFT calculations of the 300 lowest energy excited states, with results presented in Figure S19. The UV/vis spectrum is accurately predicted for both molecules. The calculated CD spectrum is less accurate, reflecting the sensitivity of the predicted spectrum to variations in the intensities and linewidths of the individual transitions. However, the loss in intensity from **2** to **3** of the strong peak at approximately 220 nm and the overall intensity in the range of 50 M^{-1} cm^{-1} are accurately determined. Analysis of the HOMO-LUMO transition in the absorbance spectrum indicates that it is a metal-ligand charge transfer transition to a delocalized π orbital on the naphthalimide (Figure S23). However, this is a single transition (at 522 nm in **2**, 479 nm at **3**), which becomes concealed by overlapping transitions at shorter wavelengths. The peak at about 350 nm in both compounds arises from transitions with strong ligand-ligand charge transfer character, with electron density shifting between the naphthalimide and the dfppy ligands in agreement with the assignment given above.

Conclusions

In this paper, we reported a series of chiral octahedral cyclometalated iridium complexes of the type [Ir(C^N)$_2$(C^C:)], {(C^N) = ppy (**2**); dfppy (**3**)} featuring a naphthalimide *N*-heterocyclic carbene ligand (C^C:) = (Napthalimide-NHC). The racemic complexes *rac*-**2** and *rac*-**3** were resolved via chiral

HPLC technique into their corresponding enantiopure species *Δ*-**2** *Λ*-**2**, and *Δ*-**3**, *Λ*-**3** as confirmed by their CD curves. The luminescent properties of the racemic compounds were performed in liquid and thin films and compared to those of the enantiopure species. The VCD technique was used as a valuable tool to assign the stereochemistry of the enantiopure species. Moreover, DFT and TD-DFT studies contributed to understand and rationalize the obtained results.

Experimental

General synthetic methods

All experimental manipulations were carried out under argon using Schlenk tube techniques. Glassware was oven-dried prior to use. Solvents were obtained from same commercial sources and used without further purification. Commercially available reagents were purchased from Sigma-Aldrich, Alfa Aesar, Acros Organics, TCI Chemical, Strem or Fluorochem and used as received unless otherwise specified. NMR spectra were recorded on a Bruker Avance 400 or on a Bruker Neo 500 spectrometers, using $CDCl_3$ as solvent. Chemical shifts are reported in ppm and couplings constants *J* in hertz, multiplicity (s = singlet, d = doublet, t = triplet, q = quadruplet, sext = sextuplet, m = multiplet. NMR spectra were referenced relative to residual ^1H (7.26 ppm) multiplicity (and to the central line of ^{13}C triplet (77.1 ppm) resonances of deuterated solvent. External calibration for ^{19}F was made with $CFCl_3$ (0 ppm) as a standard. Assignment of individual resonances of compounds **2** and **3** was achieved using a combination of 1D and 2D (^1H-^1H COSY and NOESY, ^1H-^{13}C HSQC and HMBC, ^1H-^{19}F-COSY) NMR experiments. IR spectra were recorded on a Bruker Tensor 27 spectrometer equipped with a Harrick ATR instrument. IR and VCD spectra were recorded on a Jasco FSV-6000 spectrometer in CD_2Cl_2 in a 200 microns cell and at concentrations of C 0.015-0.02 M. The half-sum of the two enantiomers has been used as the baseline. ECD spectra were recorded on a JASCO-815 spectrometer.

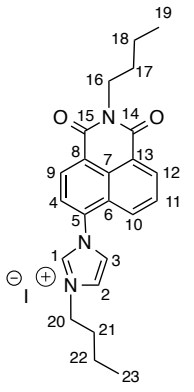

(**1**)

[4-(1'n-butyl-imidazolium)-*n*-butyl-1,8-naphthalimide]-iodide (1): A mixture of 4-(1'-imidazolyl)- *n*-butyl-1,8-naphthalimide (319 mg, 1 mmol) (200 mg, 0,66 mmol) and nBuI (2,4 mL, 19,8 mmol) was refluxed in 2ml of CH_3CN for 48 hours. The mixture was concentrated under vacuum followed by addition of Et_2O (30 mL). A light off-white precipitate appeared which was then filtered off and dried under vacuum. The product was isolated as off-white powder in 93% yield (310 mg). ^1H NMR (CDCl3, 500 MHz): δ 10.30 (t, *J* = 1.7 Hz, 1H, H1), 8.66 (dd, *J* = 7.4, 0.9 Hz, 1H, H12), 8.60 (d, *J* = 7.8 Hz, 1H, H9), 8.28 (d, *J* = 7.8 Hz, 1H, H4), 8.15 (dd, *J* = 8.5, 0.9 Hz, 1H, H10), 7.91 (dd, *J* = 8.5, 7.4 Hz, 1H, H11), 7.80 (t, *J* = 1.7 Hz, 1H, H2), 7.65 (t, *J* = 1.7 Hz, 1H, H3), 4.66 (t, *J* = 7.6 Hz, 2H, H20), 4.14 (t, *J* = 7.6 Hz, 2H, H16), 2.10 – 2.04 (m, 2H, H21), 1.72 – 1.66 (m, 2H, H17), 1.49 (sext, *J* = 7.4 Hz, 2H, H22), 1.43 (sext, *J* = 7.4 Hz, 2H, H18), 1.01 (t, *J* = 7.4 Hz, 3H, H23), 0.97 (t, *J* = 7.4 Hz, 3H, H19). ^{13}C NMR (CDCl3, 125 MHz): δ 163.2 (C14), 162.6 (C15), 137.8 (C1), 134.9 (C5), 132.6 (C12), 130.7 (C9), 129.8 (C11), 128.9 (C7), 127.6 (C10), 126.1 (C6), 126.0 (C4), 125.3 (C8), 123.9 (C3), 123.4 (C2 and C13), 51.3 (C20), 40.7 (C16), 31.9 (C21), 30.1 (C17), 20.4 (C18), 19.7 (C22), 13.9 (C19), 13.7 (C23). IR (ATR, cm^{-1}) : 2970; 1658; 1585; 1572; 1472; 1345; 1230; 1081; 869; 782; 740; 581; 432; 425; 361; 242; 201. Anal. calcd. For $C_{23}H_{26}IN_3O_2$: C 54,88; H 5,21; N 8,35. Found: C 54,62; H 5,27; N 8,22.

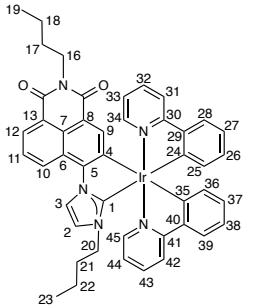

rac-**2**

***rac*-[(Ir(ppy)$_2$(*n*BuNHC-NI)] (*rac*-2)**: In a dry Schlenk tube protected from light with aluminium foil, compound 1 (64 mg, 0,128 mmol) (2.1 eq.) was loaded, followed successively by addition of degassed 1,2-dichloroethane and Ag_2O (115,5 mg, 0,501 mmol) (8.2 eq.). The mixture was stirred 5 min at room temperature. The iridium dichloro bridged dimer $[Ir(ppy)_2Cl]_2$ was added and the mixture was refluxed or heated at 110° C for 48h under argon. Then the red mixture was cooled at r.t., filtered through celite in order to remove a grey precipitate and washed with CH_2Cl_2. After evaporation of the solvents, the crude product was purified by silica gel column chromatography using a mixture of CH_2Cl_2/Et_2O (95/5). The desired fraction was then concentrated and left to stand in the freezer overnight using slow diffusion technique from either CH_2Cl_2/ Et_2O. The iridium complex *rac*-**2** was obtained as red microcrystalline solid in 80% yield. (90mg, 0.102mmol.) ^1H NMR (CDCl3, 500 MHz): δ = 8.64 (dd, *J* =8.7 Hz, *J* = 1.0 Hz, 1H, H10), 8.43 (dd, *J* = 7.3 Hz, *J* = 1.0 Hz, 1H, H12), 8.24 (s, 1H, H9), 8.20 (d, *J* = 2.2 Hz, 1H, H3), 7.90 (ddd, *J* = 5.9 Hz, *J* = 1.6 Hz, *J* = 0.7 Hz, 1H, H45), 7.87 (ddd, *J* = 5.9 Hz, *J* = 1.6 Hz, *J* = 0.7 Hz, 1H, H34), 7.84 (brd d, *J* = 8.5 Hz, 1H, H42), 7.76 (brd d, *J* = 8.6 Hz, 1H, H31), 7.69 (dd, *J* = 7.8 Hz, *J* = 1.1 Hz, 1H, H39), 7.67 - 7.65 (m, 1H, H28), 7.66 (dd, *J* = 8.7 Hz, *J* = 7.3 Hz, 1H, H11), 7.54 (ddd, *J* = 8.2 Hz, *J* = 7.3 Hz, *J* = 1.6 Hz, 1H, H43), 7.47 (ddd, *J* = 8.2 Hz, *J* = 7.4 Hz, *J* = 1.6 Hz, 1H, H32), 7.00 - 6.95 (m, 2H, H27 and H26), 6.96 (d, *J* = 2.2 Hz, 1H, H2), 6.88 (td, *J* = 7.3 Hz, *J* = 1.5 Hz, 1H, H38), 6.83 (td, *J* = 7.3 Hz, *J* = 1.4 Hz, 1H, H37), 6.67 - 6.60 (m, 3H, H33, H36 and H44), 6.38 - 6.36 (m, 1H, H25), 4.07 - 4.04 (m, 2H, H16), 3.67 (ddd, *J* = 13.1 Hz, *J* = 10.5 Hz, *J* = 5.6

Hz, 1H, H20), 3.46 (ddd, *J* = 13.1 Hz, *J* = 10.3 Hz, *J* = 5.5 Hz, 1H, H20'), 1.66 - 1.59 (m, 2H, H17), 1.43 - 1.33 (m, 2H, H18), 1.38 - 1.30 (m, 1H, H21), 1.07 - 1.00 (m, 1H, H21'), 0.92 (t, *J* = 7.4 Hz, 3H, H19), 0.85 - 0.67 (m, 2H, H22), 0.71 - 0.67 (m, 3H, H23). ^{13}C NMR (CDCl3, 125 MHz): δ = 181.7 (C1), 171.5 (C35), 170.6 (C24), 170.0 (C41), 169.2 (C30), 165.2 (C14), 164.6 (C15), 158.5 (C4), 153.6 (C45), 152.4 (C34), 148.8 (C5), 144.1 (C40), 143.8 (C9), 142.8 (C29), 134.9 (C43), 134.5 (C32), 132.7 (C36), 130.51 (C25), 130.47 (C26), 129.4 (C37), 127.60 (C12), 127.56 (C7), 125.8 (C10), 125.3 (C11), 124.6 (C28), 124.3 (C39), 123.6 (C13), 121.7 (C33 and C44), 120.8 (C27), 120.3 (C2), 120.2 (C3, C6 and C38), 119.1 (C31), 118.6 (C42), 117.8 (C8), 50.3 (C20), 40.1 (C16), 34.5 (C21), 30.3 (C17), 20.6 (C18), 19.6 (C22), 13.9 (C19), 13.8 (C23). IR (ATR, ν cm^{-1}): 2954, 1688, 1643, 1609, 1560, 1472, 1389, 1352, 1301, 1259, 1233, 1154,1112, 1051, 940, 897, 779, 759, 738, 724, 692, 629, 584, 409, 372. HRMS (ESI, m/z) : Calc. for $C_{45}H_{40}IrN_5O_2H$ [M+H$^+$] : 876,2884– Found : 876,2888

***Δ*-[(Ir(ppy)$_2$(*n*BuNHC-NI)] (*Δ*-2)**: This compound was obtained via resolution of the racemic compounds on Chiralpak IE column using heptane/ethanol/dichloromethane (80/10/10). *Δ*-**2** was first eluted on Chiralpak IE. The numbering system to assign the ^{1}H and ^{13}C chemical displacements is the same as that for the racemic compound (*rac*-2). ^{1}H NMR (CDCl3, 500 MHz): δ = 8.64 (dd, *J* =8.7 Hz, *J* = 1.0 Hz, 1H, H10), 8.43 (dd, *J* = 7.3 Hz, *J* = 1.0 Hz, 1H, H12), 8.24 (s, 1H, H9), 8.20 (d, *J* = 2.2 Hz, 1H, H3), 7.90 (ddd, *J* = 5.9 Hz, *J* = 1.6 Hz, *J* = 0.7 Hz, 1H, H45), 7.87 (ddd, *J* = 5.9 Hz, *J* = 1.6 Hz, *J* = 0.7 Hz, 1H, H34), 7.84 (brd d, *J* = 8.5 Hz, 1H, H42), 7.76 (brd d, *J* = 8.6 Hz, 1H, H31), 7.69 (dd, *J* = 7.8 Hz, *J* = 1.1 Hz, 1H, H39), 7.67 - 7.65 (m, 1H, H28), 7.66 (dd, *J* = 8.7 Hz, *J* = 7.3 Hz, 1H, H11), 7.54 (ddd, *J* = 8.2 Hz, *J* = 7.3 Hz, *J* = 1.6 Hz, 1H, H43), 7.47 (ddd, *J* = 8.2 Hz, *J* = 7.4 Hz, *J* = 1.6 Hz, 1H, H32), 7.00 - 6.95 (m, 2H, H27 and H26), 6.96 (d, *J* = 2.2 Hz, 1H, H2), 6.88 (td, *J* = 7.3 Hz, *J* = 1.5 Hz, 1H, H38), 6.83 (td, *J* = 7.3 Hz, *J* = 1.4 Hz, 1H, H37), 6.67 - 6.60 (m, 3H, H33, H36 and H44), 6.38 - 6.36 (m, 1H, H25), 4.07 - 4.04 (m, 2H, H16), 3.67 (ddd, *J* = 13.1 Hz, *J* = 10.5 Hz, *J* = 5.6 Hz, 1H, H20), 3.46 (ddd, *J* = 13.1 Hz, *J* = 10.3 Hz, *J* = 5.5 Hz, 1H, H20'), 1.66 - 1.59 (m, 2H, H17), 1.43 - 1.33 (m, 2H, H18), 1.38 -1.30 (m, 1H, H21), 1.07 - 1.00 (m, 1H, H21'), 0.92 (t, *J* = 7.4 Hz, 3H, H19), 0.85 - 0.67 (m, 2H, H22), 0.71 - 0.67 (m, 3H, H23). ^{13}C NMR (CDCl3, 125 MHz): δ = 181.7 (C1), 171.5 (C35), 170.6 (C24), 170.0 (C41), 169.2 (C30), 165.2 (C14), 164.6 (C15), 158.5 (C4), 153.6 (C45), 152.4 (C34), 148.8 (C5), 144.1 (C40), 143.8 (C9), 142.8 (C29), 134.9 (C43), 134.5 (C32), 132.7 (C36), 130.51 (C25), 130.47 (C26), 129.4 (C37), 127.60 (C12), 127.56 (C7), 125.8 (C10), 125.3 (C11), 124.6 (C28), 124.3 (C39), 123.6 (C13), 121.7 (C33 and C44), 120.8 (C27), 120.3 (C2), 120.2 (C3, C6 and C38), 119.1 (C31), 118.6 (C42), 117.8 (C8), 50.3 (C20), 40.1 (C16), 34.5 (C21), 30.3 (C17), 20.6 (C18), 19.6 (C22), 13.9 (C19), 13.8 (C23)

***Λ*-[(Ir(ppy)$_2$(*n*BuNHC-NI)] (*Λ*-2)**: This compound was obtained via resolution of the racemic compounds on Chiralpak IE column using heptane/ethanol/dichloromethane (80/10/10). *Λ*-**2** was second eluted on Chiralpak IE. The numbering system to assign the ^{1}H and ^{13}C chemical displacements is the same as that for the racemic compound (*rac*-2). ^{1}H NMR (CDCl3, 500 MHz): δ = 8.64 (dd, *J* =8.7 Hz, *J* = 1.0 Hz, 1H, H10), 8.43 (dd, *J* = 7.3 Hz, *J* = 1.0 Hz, 1H, H12), 8.24 (s, 1H, H9), 8.20 (d, *J* = 2.2 Hz, 1H, H3), 7.90 (ddd, *J* = 5.9 Hz, *J* = 1.6 Hz, *J* = 0.7 Hz, 1H, H45), 7.87 (ddd, *J* = 5.9 Hz, *J* = 1.6 Hz, *J* = 0.7 Hz, 1H, H34), 7.84 (brd d, *J* = 8.5 Hz, 1H, H42), 7.76 (brd d, *J* = 8.6 Hz, 1H, H31), 7.69 (dd, *J* = 7.8 Hz, *J* = 1.1 Hz, 1H, H39), 7.67 - 7.65 (m, 1H, H28), 7.66 (dd, *J* = 8.7 Hz, *J* = 7.3 Hz, 1H, H11), 7.54 (ddd, *J* = 8.2 Hz, *J* = 7.3 Hz, *J* = 1.6 Hz, 1H, H43), 7.47 (ddd, *J* = 8.2 Hz, *J* = 7.4 Hz, *J* = 1.6 Hz, 1H, H32), 7.00 - 6.95 (m, 2H, H27 and H26), 6.96 (d, *J* = 2.2 Hz, 1H, H2), 6.88 (td, *J* = 7.3 Hz, *J* = 1.5 Hz, 1H, H38), 6.83 (td, *J* = 7.3 Hz, *J* = 1.4 Hz, 1H, H37), 6.67 - 6.60 (m, 3H, H33, H36 and H44), 6.38 - 6.36 (m, 1H, H25), 4.07 - 4.04 (m, 2H, H16), 3.67 (ddd, *J* = 13.1 Hz, *J* = 10.5 Hz, *J* = 5.6 Hz, 1H, H20), 3.46 (ddd, *J* = 13.1 Hz, *J* = 10.3 Hz, *J* = 5.5 Hz, 1H, H20'), 1.66 - 1.59 (m, 2H, H17), 1.43 - 1.33 (m, 2H, H18), 1.38 -1.30 (m, 1H, H21), 1.07 - 1.00 (m, 1H, H21'), 0.92 (t, *J* = 7.4 Hz, 3H, H19), 0.85 - 0.67 (m, 2H, H22), 0.71 - 0.67 (m, 3H, H23). ^{13}C NMR (CDCl3, 125 MHz): δ = 181.7 (C1), 171.5 (C35), 170.6 (C24), 170.0 (C41), 169.2 (C30), 165.2 (C14), 164.6 (C15), 158.5 (C4), 153.6 (C45), 152.4 (C34), 148.8 (C5), 144.1 (C40), 143.8 (C9), 142.8 (C29), 134.9 (C43), 134.5 (C32), 132.7 (C36), 130.51 (C25), 130.47 (C26), 129.4 (C37), 127.60 (C12), 127.56 (C7), 125.8 (C10), 125.3 (C11), 124.6 (C28), 124.3 (C39), 123.6 (C13), 121.7 (C33 and C44), 120.8 (C27), 120.3 (C2), 120.2 (C3, C6 and C38), 119.1 (C31), 118.6 (C42), 117.8 (C8), 50.3 (C20), 40.1 (C16), 34.5 (C21), 30.3 (C17), 20.6 (C18), 19.6 (C22), 13.9 (C19), 13.8 (C23).

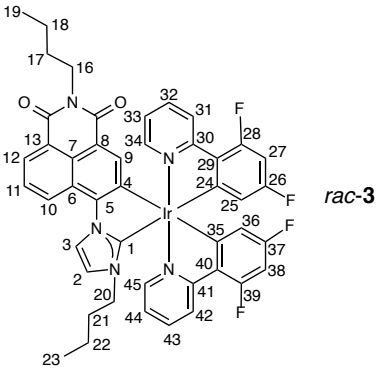

rac-3

***rac*-[(Ir(F2ppy)$_2$(*n*BuNHC-NI)] (*rac*-3)**: This complex was prepared following the experimental procedure described above for *rac*-**2**. Thus using the following starting materials and reagents: 1 (43 mg, 0,086 mmol), Ag_2O (77 mg, 0,336 mmol) and $[(F_2ppy)_2Ir(\mu\text{-}Cl)]_2$ (50 mg, 0,041 mmol) in 15 ml of degassed 1,2-dichloroethane. The target compound was isolated as red microcrystalline powder in 70% yield. ((110 mg, 0,0574 mmol). ^{1}H NMR ($CDCl_3$, 500 MHz): δ = 8.64 (dd, *J* = 8.7, *J* = 1.0 Hz, 1H, H10), 8.46 (dd, *J* = 7.3, *J* = 1.0 Hz, 1H, H12), 8.29-8.26 (m, 1H, H42), 8.24 (d, *J* = 2.2 Hz, 1H, H3), 8.22 (s, 1H, H9), 8.21-8.18 (m, 1H, H31), 7.89 (ddd, *J* = 5.9 Hz, *J* = 1.7 Hz, *J* = 0.8 Hz, 1H, H45), 7.80 (ddd, *J* = 5.9 Hz, *J* = 1.7 Hz, *J* = 0.8 Hz, 1H, H34), 7.69 (dd, *J* = 8.7 Hz, *J* = 7.3 Hz, 1H, H11), 7.63-7.59 (m, 1H, H43), 7.55-7.51 (m, 1H, H32), 7.00 (d, *J* = 2.2 Hz, 1H, H2), 6.70-6.67 (m, 1H, H33), 6.68-6.65 (m, 1H, H44), 6.46 (ddd, *J* = 12.9 Hz, *J* = 9.2 Hz, *J* = 2.4 Hz, 1H, H27), 6.40 (ddd, *J* = 12.9 Hz, *J* = 9.2 Hz, *J* = 2.4 Hz, 1H, H38), 6.03 (dd, *J* = 7.9 Hz, *J* = 2.4 Hz, 1H, H36), 5.73 (dd, *J* = 8.2 Hz, *J* = 2.4 Hz, 1H, H25), 4.09-4.05 (m, 2H, H16), 3.64 (ddd, *J* = 13.2 Hz, *J* = 10.7 Hz, *J* = 5.5 Hz, 1H, H20), 3.49 (ddd, *J* = 13.2 Hz, *J* = 10.4 Hz, *J* = 5.5 Hz, 1H, H20'),

1.68-1.61 (m, 2H, H17), 1.44-1.34 (m, 3H, H18, H21), 1.12-1.03 (m, 1H, H21'), 0.95-0.79 (m, 2H, H22), 0.93 (t, J = 7.4 Hz, 3H, H19), 0.74 (t, J = 7.2 Hz, 3H, H23). ^{13}C NMR (101 MHz, $CDCl_3$) δ 179.8 (C1), 177.2 (t, J_{CF} = 3.7 Hz, C35), 175.0 (t, J_{CF} = 3.5 Hz, C24), 166.4 (d, J_{CF} = 7.9 Hz, C41), 165.7 (d, J_{CF} = 7.9 Hz, C30), 165.0 (C14), 164.44 (C15), 164.36 (dd, J_{CF} = 257.1 Hz, J_{CF} = 11.1 Hz, C26), 164.0 (dd, J_{CF} = 257.6 Hz, J_{CF} = 10.5 Hz, C37), 162.5 (dd, J_{CF} = 262.0 Hz, J_{CF} = 11.1 Hz, C39) , 162.3 (dd, J_{CF} = 260.8 Hz, J_{CF} = 11.6 Hz, C28), 156.1 (C4), 153.5 (C45), 152.3 (C34), 148.3 (C5), 143.1 (C9), 136.1 (C43), 135.7 (C32), 128.1 (C12), 127.72 (C7) , 127.66 (C40), 126.7 (C29), 125.7 (C10 and C11), 123.6 (C13), 123.3 (d, J_{CF} = 20.7 Hz, C31), 123.0 (d, J_{CF} = 21.1 Hz, C42), 122.13 (C44), 122.10 (C33), 120.6 (C2), 120.5 (C3), 120.4 (C6), 118.3 (C8), 113.6 (dd, J_{CF} = 14.4 Hz, J_{CF} = 2.5 Hz, C36), 111.8 (dd, J_{CF} = 15.1 Hz, J_{CF} = 2.5 Hz, C25), 97.3 (t, J_{CF} = 27.0 Hz, C27), 96.6 (t, J_{CF} = 27.2 Hz, C38), 50.3 (C20), 40.2 (C16), 34.5 (C21), 30.3 (C17), 20.6 (C18), 19.7 (C22), 13.9 (C19), 13.7 (C23). ^{19}F{^{1}H}-NMR (470 MHz, CD_2Cl_2) δ = -108.95 (d, $J_{F\text{-}F}$ = 9.8 Hz, F26), -110.22 (d, $J_{F\text{-}F}$ = 9.7 Hz, F37), -110.41 (d, $J_{F\text{-}F}$ = 9.8 Hz, F28), -110.48 (d, $J_{F\text{-}F}$ = 9.7 Hz, F39). IR (ATR, cm^{-1}) : νC-H aromatique : 2960; 1693; νC-O amide : 1645; 1593; 1468; 1384; 1310; 1290; 1227; 1192; 1163; νC-N : 1100; νC-F : 1083; 972; 934; 862; 810; 779; 740; 624; 562; 441; 342; 311. HRMS (ESI, m/z) : Calc. for $C_{45}H_{36}F_4IrN_5O_2H$ [M+H$^+$] : 948,2507 – Found : 948,2518

Δ-[(Ir(F2ppy)$_2$(*n*BuNHC-NI)] (Δ-3): This compound was obtained via resolution of the racemic compounds on Chiralpak IE column using heptane/ethanol/dichloromethane (80/10/10). Δ-**3** was first eluted on Chiralpak IE. The numbering system to assign the ^{1}H and ^{13}C chemical displacements is the same as that for the racemic compound (*rac*-**3**). ^{1}H NMR ($CDCl_3$, 500 MHz): δ = 8.64 (dd, *J* = 8.7, *J* = 1.0 Hz, 1H, H10), 8.46 (dd, *J* = 7.3, *J* = 1.0 Hz, 1H, H12), 8.29-8.26 (m, 1H, H42), 8.24 (d, *J* = 2.2 Hz, 1H, H3), 8.22 (s, 1H, H9), 8.21-8.18 (m, 1H, H31), 7.89 (ddd, *J* = 5.9 Hz, *J* = 1.7 Hz, *J* = 0.8 Hz, 1H, H45), 7.80 (ddd, *J* = 5.9 Hz, *J* = 1.7 Hz, *J* = 0.8 Hz, 1H, H34), 7.69 (dd, *J* = 8.7 Hz, *J* = 7.3 Hz, 1H, H11), 7.63-7.59 (m, 1H, H43), 7.55-7.51 (m, 1H, H32), 7.00 (d, *J* = 2.2 Hz, 1H, H2), 6.70-6.67 (m, 1H, H33), 6.68-6.65 (m, 1H, H44), 6.46 (ddd, *J* = 12.9 Hz, *J* = 9.2 Hz, *J* = 2.4 Hz, 1H, H27), 6.40 (ddd, *J* = 12.9 Hz, *J* = 9.2 Hz, *J* = 2.4 Hz, 1H, H38), 6.03 (dd, *J* = 7.9 Hz, *J* = 2.4 Hz, 1H, H36), 5.73 (dd, *J* = 8.2 Hz, *J* = 2.4 Hz, 1H, H25), 4.09-4.05 (m, 2H, H16), 3.64 (ddd, *J* = 13.2 Hz, *J* = 10.7 Hz, *J* = 5.5 Hz, 1H, H20), 3.49 (ddd, *J* = 13.2 Hz, *J* = 10.4 Hz, *J* = 5.5 Hz, 1H, H20'), 1.68-1.61 (m, 2H, H17), 1.44-1.34 (m, 3H, H18, H21), 1.12-1.03 (m, 1H, H21'), 0.95-0.79 (m, 2H, H22), 0.93 (t, J = 7.4 Hz, 3H, H19), 0.74 (t, J = 7.2 Hz, 3H, H23). ^{13}C NMR (101 MHz, $CDCl_3$) δ 179.8 (C1), 177.2 (t, J_{CF} = 3.7 Hz, C35), 175.0 (t, J_{CF} = 3.5 Hz, C24), 166.4 (d, J_{CF} = 7.9 Hz, C41), 165.7 (d, J_{CF} = 7.9 Hz, C30), 165.0 (C14), 164.44 (C15), 164.36 (dd, J_{CF} = 257.1 Hz, J_{CF} = 11.1 Hz, C26), 164.0 (dd, J_{CF} = 257.6 Hz, J_{CF} = 10.5 Hz, C37), 162.5 (dd, J_{CF} = 262.0 Hz, J_{CF} = 11.1 Hz, C39) , 162.3 (dd, J_{CF} = 260.8 Hz, J_{CF} = 11.6 Hz, C28), 156.1 (C4), 153.5 (C45), 152.3 (C34), 148.3 (C5), 143.1 (C9), 136.1 (C43), 135.7 (C32), 128.1 (C12), 127.72 (C7) , 127.66 (C40), 126.7 (C29), 125.7 (C10 and C11), 123.6 (C13), 123.3 (d, J_{CF} = 20.7 Hz, C31), 123.0 (d, J_{CF} = 21.1 Hz, C42), 122.13 (C44), 122.10 (C33), 120.6 (C2), 120.5 (C3), 120.4 (C6), 118.3 (C8), 113.6 (dd, J_{CF} = 14.4 Hz, J_{CF} = 2.5 Hz, C36), 111.8 (dd, J_{CF} = 15.1 Hz, J_{CF} = 2.5 Hz, C25), 97.3 (t, J_{CF} = 27.0 Hz, C27), 96.6 (t, J_{CF} = 27.2 Hz, C38), 50.3 (C20), 40.2 (C16), 34.5 (C21), 30.3 (C17), 20.6 (C18), 19.7 (C22), 13.9 (C19), 13.7 (C23). ^{19}F{^{1}H}-NMR (470 MHz, CD_2Cl_2) δ = -108.95 (d, $J_{F\text{-}F}$ = 9.8 Hz, F26), -110.22 (d, $J_{F\text{-}F}$ = 9.7 Hz, F37), -110.41 (d, $J_{F\text{-}F}$ = 9.8 Hz, F28), -110.48 (d, $J_{F\text{-}F}$ = 9.7 Hz, F39).).

Λ-[(Ir(F2ppy)$_2$(*n*BuNHC-NI)] (Λ-3): This compound was obtained via resolution of the racemic compounds on Chiralpak IE column using heptane/ethanol/dichloromethane (80/10/10). Λ-**3** was second eluted on Chiralpak IE. The numbering system to assign the ^{1}H and ^{13}C chemical displacements is the same as that for the racemic compound (*rac*-**3**). ^{1}H NMR ($CDCl_3$, 500 MHz): δ = 8.64 (dd, *J* = 8.7, *J* = 1.0 Hz, 1H, H10), 8.46 (dd, *J* = 7.3, *J* = 1.0 Hz, 1H, H12), 8.29-8.26 (m, 1H, H42), 8.24 (d, *J* = 2.2 Hz, 1H, H3), 8.22 (s, 1H, H9), 8.21-8.18 (m, 1H, H31), 7.89 (ddd, *J* = 5.9 Hz, *J* = 1.7 Hz, *J* = 0.8 Hz, 1H, H45), 7.80 (ddd, *J* = 5.9 Hz, *J* = 1.7 Hz, *J* = 0.8 Hz, 1H, H34), 7.69 (dd, *J* = 8.7 Hz, *J* = 7.3 Hz, 1H, H11), 7.63-7.59 (m, 1H, H43), 7.55-7.51 (m, 1H, H32), 7.00 (d, *J* = 2.2 Hz, 1H, H2), 6.70-6.67 (m, 1H, H33), 6.68-6.65 (m, 1H, H44), 6.46 (ddd, *J* = 12.9 Hz, *J* = 9.2 Hz, *J* = 2.4 Hz, 1H, H27), 6.40 (ddd, *J* = 12.9 Hz, *J* = 9.2 Hz, *J* = 2.4 Hz, 1H, H38), 6.03 (dd, *J* = 7.9 Hz, *J* = 2.4 Hz, 1H, H36), 5.73 (dd, *J* = 8.2 Hz, *J* = 2.4 Hz, 1H, H25), 4.09-4.05 (m, 2H, H16), 3.64 (ddd, *J* = 13.2 Hz, *J* = 10.7 Hz, *J* = 5.5 Hz, 1H, H20), 3.49 (ddd, *J* = 13.2 Hz, *J* = 10.4 Hz, *J* = 5.5 Hz, 1H, H20'), 1.68-1.61 (m, 2H, H17), 1.44-1.34 (m, 3H, H18, H21), 1.12-1.03 (m, 1H, H21'), 0.95-0.79 (m, 2H, H22), 0.93 (t, J = 7.4 Hz, 3H, H19), 0.74 (t, J = 7.2 Hz, 3H, H23). ^{13}C NMR (101 MHz, $CDCl_3$) δ 179.8 (C1), 177.2 (t, J_{CF} = 3.7 Hz, C35), 175.0 (t, J_{CF} = 3.5 Hz, C24), 166.4 (d, J_{CF} = 7.9 Hz, C41), 165.7 (d, J_{CF} = 7.9 Hz, C30), 165.0 (C14), 164.44 (C15), 164.36 (dd, J_{CF} = 257.1 Hz, J_{CF} = 11.1 Hz, C26), 164.0 (dd, J_{CF} = 257.6 Hz, J_{CF} = 10.5 Hz, C37), 162.5 (dd, J_{CF} = 262.0 Hz, J_{CF} = 11.1 Hz, C39) , 162.3 (dd, J_{CF} = 260.8 Hz, J_{CF} = 11.6 Hz, C28), 156.1 (C4), 153.5 (C45), 152.3 (C34), 148.3 (C5), 143.1 (C9), 136.1 (C43), 135.7 (C32), 128.1 (C12), 127.72 (C7) , 127.66 (C40), 126.7 (C29), 125.7 (C10 and C11), 123.6 (C13), 123.3 (d, J_{CF} = 20.7 Hz, C31), 123.0 (d, J_{CF} = 21.1 Hz, C42), 122.13 (C44), 122.10 (C33), 120.6 (C2), 120.5 (C3), 120.4 (C6), 118.3 (C8), 113.6 (dd, J_{CF} = 14.4 Hz, J_{CF} = 2.5 Hz, C36), 111.8 (dd, J_{CF} = 15.1 Hz, J_{CF} = 2.5 Hz, C25), 97.3 (t, J_{CF} = 27.0 Hz, C27), 96.6 (t, J_{CF} = 27.2 Hz, C38), 50.3 (C20), 40.2 (C16), 34.5 (C21), 30.3 (C17), 20.6 (C18), 19.7 (C22), 13.9 (C19), 13.7 (C23). ^{19}F{^{1}H}-NMR (470 MHz, CD_2Cl_2) δ = -108.95 (d, $J_{F\text{-}F}$ = 9.8 Hz, F26), -110.22 (d, $J_{F\text{-}F}$ = 9.7 Hz, F37), -110.41 (d, $J_{F\text{-}F}$ = 9.8 Hz, F28), -110.48 (d, $J_{F\text{-}F}$ = 9.7 Hz, F39).

Photophysical measurements. Spectrofluorimetric grade acetonitrile (Merck Uvasol®) was used to prepare the solutions of the six compounds. In the luminescence experiments, the solutions were put into fluorimetric Suprasil quartz gas-tight cuvettes (1 cm) and deoxygenated for 20 minutes by bubbling argon. The absorption spectra were recorded on a Perkin-Elmer Lambda 950 spectrophotometer. The emission spectra were collected with an Edinburgh Instruments FLS920 spectrometer equipped with a Peltier-cooled Hamamatsu R928P photomultiplier tube (185–900 nm) and the spectra were corrected by a calibration curve supplied with the

instrument. The photoluminescence quantum yields (ϕ) of the eight compounds in solution were determined from the corrected emission spectra, using an air-equilibrated water solution of quinine sulfate in 1 N H_2SO_4 as reference (ϕ = 0.546).[9] The emission spectra of powder samples were recorded in front-face mode with the same fluorimeter. The excited state lifetimes (τ) were measured by the time-correlated single photon counting (TCSPC) technique on an HORIBA FluoroHub system, equipped with a pulsed NanoLED (λ_{exc} = 465 nm) and with a TBX-05C Picosecond Photon Detection Module (300-850 nm).

Computational details.

Geometries of **2** and **3** were initially optimized in B3LYP/LANL2DZ calculations with no solvent model. These geometries were then used as starting points for geometry optimizations with the larger cc-pVDZ basis set and using the COSMO solvation model. Geometries were independently optimized with solvent parameters for dichloromethane, in order to model the experimental IR and VCD spectra, and for acetonitrile, to model the electronic spectra. TD-DFT calculations to find the excitation energies of the lowest 300 states were carried out at the optimized ground state geometries to simulate the electronic UV/vis and CD spectra. Simulated spectra assume linewidths of 5 cm^{-1} for IR/VCD spectra and 0.25 eV for UV/vis/CD spectra.

Acknowledgements

Sorbonne Université-Campus Pierre et Marie Curie, CNRS and Ile de France region for financial support of the 500 MHz NMR spectrometer to Chimie Paristech are gratefully acknowledged. ALC acknowledges support from NSF OAC-2019194. A. B. acknowledges support from National Research Council, Italy, CNR SAC.AD002.027.

References

1. L. Flamigni, A. Barbieri, C. Sabatini, B. Ventura and F. Barigelletti, in *Photochemistry and Photophysics of Coordination Compounds Ii*, 2007, vol. 281, pp. 143-203.
2. Y. You and W. Nam, *Chem. Soc. Rev.*, 2012, **41**, 7061-7084.
3. J. Lee, H.-F. Chen, T. Batagoda, C. Coburn, P. I. Djurovich, M. E. Thompson and S. R. Forrest, *Nat. Mater.*, 2016, **15**, 92-98.
4. G. DiMarco, M. Lanza, M. Pieruccini and S. Campagna, *Adv. Mater.*, 1996, **8**, 576-&.
5. Y. Amao, Y. Ishikawa and I. Okura, *Anal. Chim. Acta*, 2001, **445**, 177-182.
6. M. C. DeRosa, P. J. Mosher, G. P. A. Yap, K. S. Focsaneanu, R. J. Crutchley and C. E. B. Evans, *Inorg. Chem.*, 2003, **42**, 4864-4872.
7. K. K.-W. Lo, K. H.-K. Tsang, K.-S. Sze, C.-K. Chung, T. K.-M. Lee, K. Y. Zhang, W.-K. Hui, C.-K. Li, J. S.-Y. Lau, D. C.-M. Ng and N. Zhu, *Coord. Chem. Rev.*, 2007, **251**, 2292-2310.
8. K. A. King, P. J. Spellane and R. J. Watts, *J. Am. Chem. Soc.*, 1985, **107**, 1431-1432.
9. M. Montalti, A. Credi, L. Prodi and M. T. Gandolfi, *Handbook of Photochemistry*, CRC Press, 3rd edn., 2006.
10. A. Bonfiglio and M. Mauro, *Eur. J. Inorg. Chem.*, 2020, DOI: 10.1002/ejic.202000509, 3427-3442.
11. A. Ehnbom, S. K. Ghosh, K. G. Lewis and J. A. Gladysz, *Chem. Soc. Rev.*, 2016, **45**, 6799-6811.
12. A. R. Wegener, C. Q. Kabes and J. A. Gladysz, *Acc. Chem. Res.*, 2020, **53**, 2299-2313.
13. S. Y. Yao, Y. L. Ou and B. H. Ye, *Inorg. Chem.*, 2016, **55**, 6018-6026.
14. T. von Arx, A. Szentkuti, T. N. Zehnder, O. Blacque and K. Venkatesan, *J. Mat. Chem. C*, 2017, **5**, 3765-3769.
15. L. P. Li, H. L. Peng and B. H. Ye, *Inorg. Chem.*, 2019, **58**, 12245-12253.
16. E. Meggers, *Eur. J. Inorg. Chem.*, 2011, DOI: 10.1002/ejic.201100327, 2911-2926.
17. X. Huang and E. Meggers, *Acc. Chem. Res.*, 2019, **52**, 833-847.
18. N. Hellou, M. Srebro-Hooper, L. Favereau, F. Zinna, E. Caytan, L. Toupet, V. Dorcet, M. Jean, N. Vanthuyne, J. A. G. Williams, L. Di Bari, J. Autschbach and J. Crassous, *Angew. Chem., Int. Ed.*, 2017, **56**, 8236-8239.
19. A. Mace, N. Hellou, J. Hammoud, C. Martin, E. S. Gauthier, L. Favereau, T. Roisnel, E. Caytan, G. Nasser, N. Vanthuyne, J. A. G. Williams, F. Berree, B. Carboni and J. Crassous, *Helv. Chim. Acta*, 2019, **102**, n/a.
20. E. S. Gauthier, N. Hellou, E. Caytan, S. Del Fre, V. Dorcet, N. Vanthuyne, L. Favereau, M. Srebro-Hooper, J. A. G. Williams and J. Crassous, *Inorg. Chem. Front.*, 2021, **8**, 3916-3925.
21. D. R. Martir, C. Momblona, A. Pertegas, D. B. Cordes, A. M. Z. Slawin, H. J. Bolink and E. Zysman-Colman, *Acs Applied Materials & Interfaces*, 2016, **8**, 33907-33915.
22. H. Sesolis, J. Dubarle-Offner, C. K. M. Chan, E. Puig, G. Gontard, P. Winter, A. L. Cooksy, V. W. W. Yam and H. Amouri, *Chem. - Eur. J.*, 2016, **22**, 8032-8037.
23. P.-H. Lanoe, J. Chan, G. Gontard, F. Monti, N. Armaroli, A. Barbieri and H. Amouri, *Eur. J. Inorg. Chem.*, 2016, 1631-1634.
24. P. H. Lanoe, B. Najjari, F. Hallez, G. Gontard and H. Amouri, *Inorganics*, 2017, **5**, 58.

25. P. H. Lanoe, J. Chan, A. Groue, G. Gontard, A. Jutand, M. N. Rager, N. Armaroli, F. Monti, A. Barbieri and H. Amouri, *Dalton Trans.*, 2018, **47**, 3440-3451.
26. S. Banerjee, E. B. Veale, C. M. Phelan, S. A. Murphy, G. M. Tocci, L. J. Gillespie, D. O. Frimannsson, J. M. Kelly and T. Gunnlaugsson, *Chem. Soc. Rev.*, 2013, **42**, 1601-1618.
27. G. Pescitelli, S. Luedeke, A.-C. Chamayou, M. Marolt, V. Justus, M. Gorecki, L. Arrico, L. Di Bari, M. A. Islam, I. Gruber, M. Enamullah and C. Janiak, *Inorg. Chem.*, 2018, **57**, 13397-13408.
28. M. Gorecki, M. Enamullah, M. A. Islam, M. K. Islam, S.-P. Hofert, D. Woschko, C. Janiak and G. Pescitelli, *Inorg. Chem.*, 2021, DOI: 10.1021/acs.inorgchem.1c01503
29. L. A. Nafie, *Infrared Vibrational Optical Activity: Measurement and Instrumentation. in Comprehensive Chiroptical Spectroscopy*, Wiley-VCH, 2012.
30. C. Citti, U. M. Battisti, G. Ciccarella, V. Maiorano, G. Gigli, S. Abbate, G. Mazzeo, E. Castiglioni, G. Longhi and G. Cannazza, *Journal of Chromatography A*, 2016, **1467**, 335-346.
31. T. Taniguchi and K. Monde, *J. Am. Chem. Soc.*, 2012, **134**, 3695-3698.
32. G. Mazzeo, M. Fuse, G. Longhi, I. Rimoldi, E. Cesarotti, A. Crispini and S. Abbate, *Dalton Trans.*, 2016, **45**, 992-999.
33. R. Manguin, D. Pichon, R. Tarrieu, T. Vives, T. Roisnel, V. Dorcet, C. Crevisy, K. Miqueu, L. Favereau, J. Crassous, M. Mauduit and O. Basle, *Chem. Commun.*, 2019, **55**, 6058-6061.
34. A. D. Becke, *Physical Review A*, 1988, **38**, 3098-3100.
35. A. D. Becke, *Journal of Chemical Physics*, 1993, **98**, 1372-1377.
36. C. T. Lee, W. T. Yang and R. G. Parr, *Physical Review B*, 1988, **37**, 785-789.
37. T. H. Dunning, *Journal of Chemical Physics*, 1989, **90**, 1007-1023.
38. M. J. Frisch, G. W. Trucks, H. B. Schlegel, G. E. Scuseria, M. A. Robb, J. R. Cheeseman, G. Scalmani, V. Barone, G. A. Petersson, H. Nakatsuji, X. Li, M. Caricato, A. V. Marenich, J. Bloino, B. G. Janesko, R. Gomperts, B. Mennucci, H. P. Hratchian, J. V. Ortiz, A. F. Izmaylov, J. L. Sonnenberg, Williams, F. Ding, F. Lipparini, F. Egidi, J. Goings, B. Peng, A. Petrone, T. Henderson, D. Ranasinghe, V. G. Zakrzewski, J. Gao, N. Rega, G. Zheng, W. Liang, M. Hada, M. Ehara, K. Toyota, R. Fukuda, J. Hasegawa, M. Ishida, T. Nakajima, Y. Honda, O. Kitao, H. Nakai, T. Vreven, K. Throssell, J. A. Montgomery Jr, J. E. Peralta, F. Ogliaro, M. J. Bearpark, J. J. Heyd, E. N. Brothers, K. N. Kudin, V. N. Staroverov, T. A. Keith, R. Kobayashi, J. Normand, K. Raghavachari, A. P. Rendell, J. C. Burant, S. S. Iyengar, J. Tomasi, M. Cossi, J. M. Millam, M. Klene, C. Adamo, R. Cammi, J. W. Ochterski, R. L. Martin, K. Morokuma, O. Farkas, J. B. Foresman and D. J. Fox, *Journal*, 2016.
39. S. Chiodo, N. Russo and E. Sicilia, *Journal of Chemical Physics*, 2006, **125**.

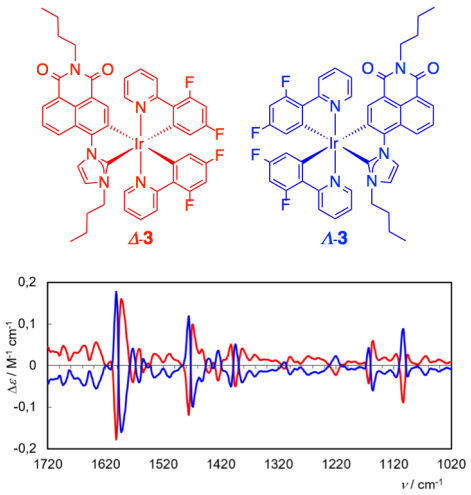

Chiral cyclometalated iridium complexes [Ir(N^C)2(C^C:)] displaying *N*-heterocyclic carbene-naphthalimide chromophore are described. At room temperature they act as emitters in the red and NIR regions. A combination of several spectroscopic techniques to investigate their optical and chiroptical properties is performed. Remarkably VCD technique and TD-DFT allow us to ascertain their stereochemistry as shown for **Δ-3** and **Λ-3** enantiomers.